FINAL TECHNICAL REPORT

USGS AWARD G12AP20006

Modeling Interaction of Slip Phenomena in Parkfield

Principal Investigator: Nadia Lapusta, California Institute of Technology
1200 E. California Blvd., Pasadena, CA 91125
(626) 395-2277, Fax: (626) 568-2719, lapusta@caltech.edu

Abstract

The Parkfield section of the San Andreas fault is a well-instrumented natural laboratory that displays the full range of fault slip behaviors: relatively large, M6, events, small repeating earthquakes, seismic tremors, and creeping regions. We have developed a fully dynamic model of the Parkfield segment based on full elastodynamics and laboratory-based friction laws. The model succeeds in reproducing a realistic earthquake sequence of irregular M 6.0 earthquakes - including events similar to the ones in 1966 and 2004 - and provides an excellent match for the detailed interseismic, coseismic, and postseismic observations collected along this fault during the most recent M 6.0 earthquake and surrounding interseismic periods. The model will serve as the base point for future improvements, including incorporation of enhanced dynamic weakening and interaction with a more realistic model of a nearby creeping segment and its well-studied repeating earthquake sequences.

We have also focused on the broader question of seismic vs. aseismic slip. Faults experience both slow slip and fast, seismic-wave producing, rupture events perceived as earthquakes. These behaviors are often assumed to be separated in space and to occur on two different types of fault segments: one with stable, rate-strengthening, friction and the other with rate-weakening friction that leads to stick-slip. The unexpected Mw 9.0 2011 Tohoku-Oki earthquake shook such assumptions by accumulating its largest seismic slip in the area that had been assumed to be creeping. Our group has developed a model in which stable, rate-strengthening behavior at low slip rates is combined with coseismic weakening, allowing unstable slip to occur in segments which can also creep between events. The model parameters are based on laboratory measurements on samples from the fault of the Mw 7.6 1999 Chi-Chi earthquake. The long-term slip behavior of the model - examined using the state-of-the-art numerical approach that includes all wave effects - reproduces and explains a number of both long-term and coseismic observations about faults that hosted the Tohoku-Oki and Chi-Chi earthquakes.

The implication that earthquake rupture may break through large portions of creeping segments - currently perceived as barriers - requires re-evaluation of seismic hazard in many areas, including California. It motivates us to investigate the possibility for large earthquakes to penetrate below the seismogenic zone (as defined through microseismicity distribution), into the deeper, creeping fault extensions, the subject of our ongoing study. Our modeling efforts so far indeed support such a scenario, further indicating that such deeper penetration in past events can be detected by the absence of concentrated microseismicity at the bottom of the seismogenic zone.

From a more general point of view, the studies have advanced our understanding of the types of frictional behavior relevant to fault slip. Our studies of the penetration depth of large events contribute to the evaluation of seismic hazard in California and other areas. The resulting better understanding of seismic hazard and physics of large destructive events contributes to reduction of losses from earthquakes in the US.

Publications and presentations supported by this project:

Noda, H. and N. Lapusta, Stable creeping fault segments can become destructive as a result of dynamic weakening, *Nature* **493**, 518-521, 2013.

Barbot, S., N. Lapusta, and J.-P. Avouac, Under the hood of the earthquake machine: Toward predictive modeling of the seismic cycle, *Science*, **336** (6082), pp. 707-710, 2012.

Jiang, J., and N. Lapusta, Detecting Penetration of Large Earthquake Ruptures Below the Seismogenic Zone Using Microseismicity, *Seismological Society of America Annual Meeting*, Apr. 2013.

Jiang, J., and N. Lapusta, Do Large Earthquakes Penetrate below the Seismogenic Zone? Potential Clues from Microseismicity, *AGU Fall Meeting*, San Francisco, CA, USA, Dec., 2012. (Oral Presentation)

Jiang, J., and N. Lapusta, Do Large Earthquakes Penetrate below the Seismogenic Zone? Potential Clues from Microseismicity, *2012 SCEC Annual Meeting*, Palm Springs, CA, USA, Sept. 2012.

Lapusta, N., Models of Earthquakes and Aseismic Slip Based on Laboratory-Derived Friction Laws: Accomplishments and Future Challenges, *Seismological Society of America Annual Meeting*, Apr. 2013. (Invited oral presentation)

Fully dynamic model of the M 6.0 earthquake sequences at Parkfield

We have built the first fully dynamic model of the Parkfield fault segment that quantitatively reproduces its behavior over the entire earthquake cycle (Barbot et al., 2012; Figure 1). In the model, a rate-and-state fault is tuned to the wealth of data for the Parkfield segment of the San Andreas Fault. The model succeeds in reproducing a realistic earthquake sequence of irregular Mw 6 mainshocks - including events similar to the ones in 1966 and 2004 - and provides an excellent match to the detailed inter-, co-, and post-seismic observations during the most recent earthquake cycle. The model is based in rate-and-state friction (see the following section). Such calibrated physical models may be used in the future to assess seismic hazard and forecast seismicity response to perturbations of natural or anthropogenic origins.

In particular, this model will enable us to investigate the interaction between the seismogenic Parkfield segment and the nearby creeping one. One can study whether the creeping segment of the SAF next to Parkfield, currently perceived as a barrier to earthquake rupture, may succumb to dynamic weakening, potentially resulting in a massive earthquake that would involve the entire California, from San Diego and Los Angeles to San Francisco. Such possibility follows from our research (Noda and Lapusta, 2013) detailed in the next section of this report. One can also study how the seismic and postseismic slip from the Parkfield segment interacts with the repeating sequences in the creeping segments. For example, some repeating sequences shut down after the 2004 M6 event, and some of them now come back to producing earthquakes (Nadeau, personal communication). These sequences are located close to the area of the coseismic slip of the 2004 M6 event. The model of the two segments, refined in the places of interest with respect to friction properties, will be able to investigate the reasons for such behavior. Our hypothesis is that coseismic slip penetration in places of some repeating earthquakes relieves stress there, stops creep for a period of time, and hence shuts down the repeaters there.

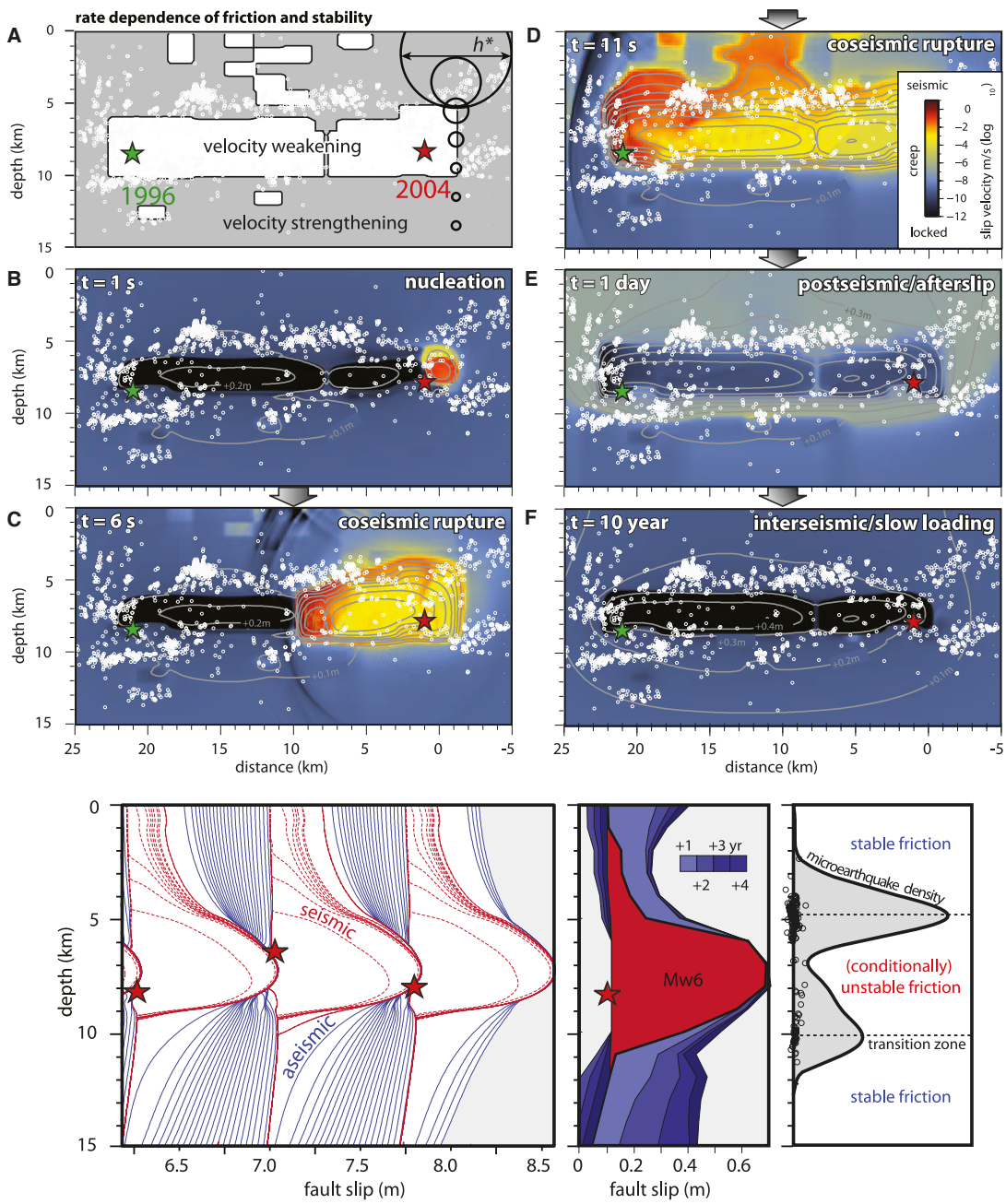

Figure 1. (Top three rows) Model that reproduces the large-scale behavior of Parkfield (from Barbot et al., 2012). (A) Spatial distribution of VW (white) and VS (gray) friction properties ($a - b$), with VW values in the seismogenic zone (SZ) delineated by the background seismicity, a few shallow patches required to explain near-field GPS data, and two deeper patches included for illustration purposes. (B) to (F) Snapshots of a M_W 6.0 earthquake and associated slow slip, with rupture nucleating spontaneously near the 2004 earthquake hypocenter (B), propagating to the north and rupturing the entire SZ (C-D), followed by postseismic slip (E) and interseismic loading of the partially locked SZ (F). Such M_W 6.0 events occur ~20 years apart, with some irregularity. (Bottom) Depth profiles through the middle of the SZ comparing the modeled history of fault slip for three events (left) to the one (right) inferred from the inversions of InSAR and GPS data in the period 1999 to 2010 (Barbot et al., 2012). The red stars indicate the location of hypocenters.

Physical model for seismic slip in creeping regions and its success for Tohoku-Oki and Chi-Chi

Our model includes two aspects of earthquake source physics that have been gaining acceptance and validation through laboratory experiments and comparison of earthquake models with observations. The first one is the rate-and-state nature of fault friction at low, aseismic slip rates, conclusively documented in laboratory experiments and used to reproduce, both qualitatively and quantitatively, a number of earthquake-source observations (Dieterich, 2007; Scholz, 1998). Our previous studies supported by USGS have shown that the standard logarithmic rate and state formulations (Dieterich, 1979, 1981; Ruina, 1983; Blanpied et al., 1991, 1995) already allow us to match a number of basic observations regarding the Parkfield segment behavior (Chen and Lapusta, 2009; Chen et al., 2010; Barbot et al., 2012). Such laws express the dependence of frictional shear strength τ_f on the effective normal stress $\bar{\sigma}$, slip rate V (which we also call slip velocity), and evolving properties (state) of the contact population represented by the state variable θ, through:

$$\tau_f = \bar{\sigma} f = (\sigma - p)[f_o + a\ln(V/V_o) + b\ln(V_o\theta/L)],$$
$$\frac{\partial\theta}{\partial t} = 1 - \frac{V\theta}{L} \text{ or } \frac{\partial\theta}{\partial t} = -\frac{V\theta}{L}\ln\frac{V\theta}{L} \text{ or } \frac{\partial\theta}{\partial t} = \exp\left(-\frac{V}{V_c}\right) - \frac{V\theta}{L}\ln\frac{V\theta}{L}, \quad (1)$$

where σ is the normal traction, p is the pore pressure, f_o, V_o, a, b, and L are rate and state parameters, with L being the characteristic slip for state variable evolution, and V_c is the cut-off velocity of the order of 10^{-8} m/s. In these laws, the rate and state features result in small variations (of the order of 1-10%) from the baseline frictional strength given by $\bar{\sigma} f_o$. Despite being small, these variations are fundamentally important for physically and mathematically meaningful stability properties of frictional sliding (e.g., Rice, Lapusta, and Ranjith, 2001). In the steady state, $(a - b)$ is the rate-and-state parameter that can be used to model both stable, rate-strengthening fault segments ($a - b > 0$) and potentially seismic, rate-weakening fault segments ($a - b < 0$).

The second emerging property of the earthquake source is additional substantial fault weakening at seismic slip rates. While theories of such weakening have a long history (Sibson, 1973), relatively recent laboratory confirmations of this phenomenon (Tsutsumi and Shimamoto, 1997; Tullis, 2007) have put this notion on the earthquake science map. Our prior support from USGS and NSF has enabled us to incorporate shear heating dynamic weakening mechanisms, such as flash heating and thermal pressurization, into our simulations of earthquake cycles (e.g., Noda and Lapusta, 2010, 2013). One shear-heating weakening mechanism that has laboratory support is flash heating (e.g., Rice, 1999, Goldsby and Tullis, 2003, Beeler and Tullis, 2003, Rice, 2006, Beeler et al. 2008), in which tips of contacting fault gouge grains heat up and weaken. Such weakening can be activated even for very small slips of the order of 100 microns if the shear strain rate is high enough. Hence this mechanism can be important even for the smallest earthquakes. Another relevant mechanism is pore fluid pressurization (e.g., Sibson, 1973; Andrews, 2002; Noda, 2004; Bizzarri and Cocco, 2006a,b; Rice, 2006; Noda et al., 2009), in which rapid shearing raises the temperature and hence pore fluid pressure, lowering the

effective normal stress and hence the frictional resistance. To include flash heating and/or pore pressurization into our models, we modify the logarithmic rate and state formulation (1) to

$$\tau_f = \bar{\sigma} f = (\sigma - p)\left[\frac{f_o - f_w + a\ln(V/V_o) + b\ln(V_o\theta/L)}{1 + L/\theta V_w} + f_w\right], \tag{4}$$

where V_w is the characteristic slip velocity at which flash heating starts to operate, f_w is the residual friction coefficient, and pore pressure p could be evolving due to shear heating as discussed below. Based on laboratory experiments and flash heating theories, V_w is of the order of 0.1 m/s. Selecting much larger values of V_w than the seismic slip rates of the order of 1-10 m/s would effectively disable the additional weakening due to flash heating. The coupled temperature and pore pressure evolution is calculated by (Rice, 2006 and references therein, Noda et al., 2009, Noda and Lapusta, 2010):

$$\frac{\partial T}{\partial t} = \alpha_{th}\frac{\partial^2 T}{\partial y^2} + \frac{\omega(y)}{\rho c}, \quad \frac{\partial p}{\partial t} = \alpha_{hy}\frac{\partial^2 p}{\partial y^2} + \Lambda\frac{\partial T}{\partial t}, \tag{5}$$

where y is the space coordinate normal to the fault, T is the temperature, α_{th} and α_{th} are the thermal and hydraulic diffusivities, $\omega(y)$ is the heat generation rate the integral of which over the width w of the shearing layer equals to $\tau_f V$, ρc is the specific heat, Λ is pore pressure change per unit temperature change under undrained condition. (Note that this formulation can also include inelastic dilatancy, as an additional term in the equation for the pore pressure evolution.) The heat source, $\omega(y)$, is distributed in a narrow shear zone around the fault. The standard assumption is to take this term to represent the effect of uniform sliding in the fault zone of thickness w.

In our simulations, spontaneous long-term slip history of fault slip is determined using the 3D simulation methodology of Lapusta and Liu (2009) and Noda and Lapusta (2010), which is the extension of the 2D methodology of Lapusta et al. (2000). The methodology incorporates slow tectonic-type loading and all dynamic effects of self-driven dynamic rupture. The algorithm allows us to treat accurately long deformation histories and to calculate, for each earthquake episode, initially quasi-static accelerating slip (nucleation process), the following dynamic rupture break-out and propagation, postseismic response, and ongoing slippage throughout the loading period in creeping fault region.

To obtain seismic slip in a "creeping" region, our fault model incorporates a patch that combines stable, rate-strengthening properties at low slip rates with substantial coseismic weakening. While the combination of rate-and-state friction with enhanced dynamic (or co-seismic) weakening for stick-slip regions have been explored in a number of studies, the idea of studying enhanced co-seismic weakening in velocity-strengthening regions at low slip rates (which can creep due to plate loading) is very recent. It has first been explored in our group (Noda and Lapusta, Nature, 2013) with application to the Mw 9.0 2011 Tohoku-Oki and Mw 7.6 1999 Chi-Chi earthquakes. Studying such regions is motivated by laboratory measurements (Tanikawa and Shimamoto, 2009) on samples from the Chelungpu fault in Taiwan that hosted the 1999 Mw 7.6 Chi-Chi earthquake, one of the most well-studied events (Tanikawa and Shimamoto, 2009; Ma et al., 2000, 2003). Chi-Chi's fault rupture nucleated in the southern region of the Chelungpu fault and propagated mainly to the north, where it accumulated its

largest coseismic slip of about 8 m (Figure 2b). However, the southern region of substantially lower slip generated more high-frequency radiation (Ma et al., 2000, 2003). Laboratory measurements (Tanikawa and Shimamoto, 2009) on rock samples from two shallow boreholes that penetrated the Chelungpu fault indicate that, at low slip rates, the southern fault region has earthquake-prone rate-weakening friction ($a - b < 0$), while the northern region has stable, rate-strengthening friction ($a - b > 0$). However, the rock permeability is lower in the north by about two orders of magnitude (Tanikawa and Shimamoto, 2009), indicating that the northern part of the fault is more susceptible to coseismic weakening by thermal pressurization of pore fluids. Motivated by these measurements, our model in the Chi-Chi-related study considered the interaction of two patches, A and B, with the corresponding laboratory-measured properties (Figure 2; Noda and Lapusta, 2013).

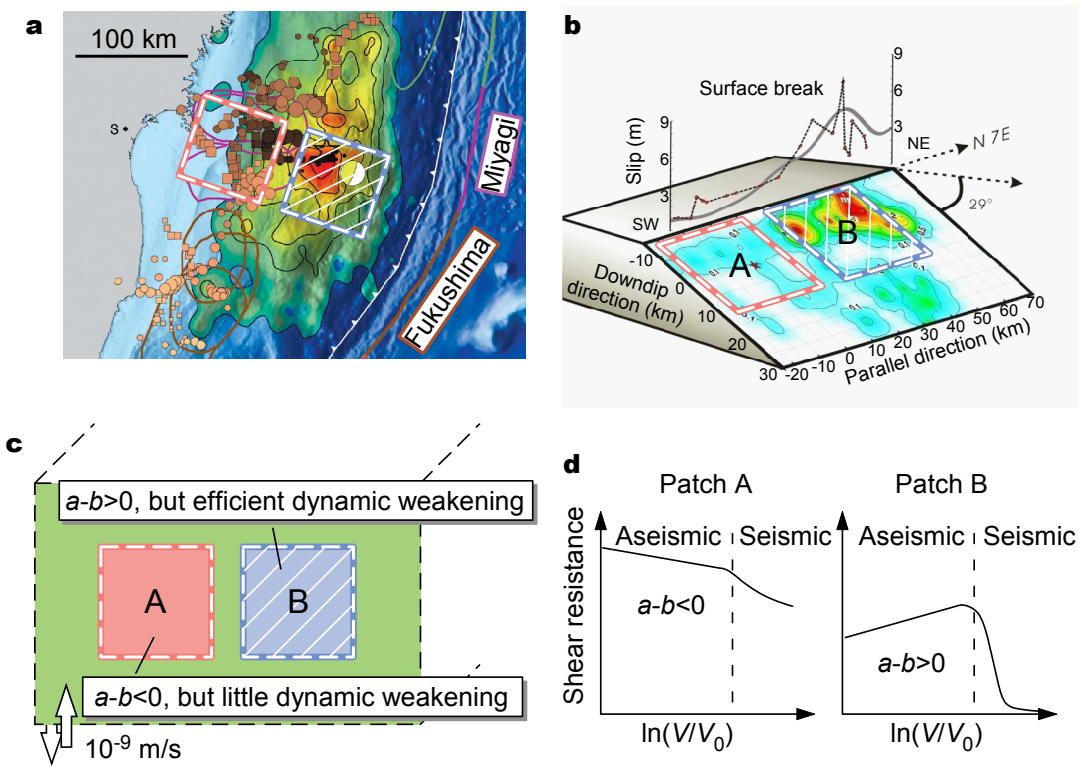

Figure 2. Schematics of the fault model of Noda and Lapusta (2013) and its correspondence to great earthquakes. (a-b) Slip distributions in 2011 Tohoku-Oki (Simons et al., 2011) and 1999 Chi-Chi (Ma et al., 2003) earthquakes. They featured a larger-slip patch producing lower high-frequency radiation than the neighboring lower-slip patch. The white squares outline the patches of our model. (c) Fault model motivated by experimental studies (Tanikawa and Shimamoto, 2009) for the Chelungpu fault that hosted Chi-Chi earthquake. At aseismic slip rates, patch A has instability-prone rate-weakening friction while patch B has stable rate-strengthening friction. However, patch B is more susceptible to coseismic weakening. (d) The schematics of how shear resistance in the patches depends on their slip rate.

The resulting model response in terms of earthquake sequences and slow slip qualitatively reproduces a range of observations for both Chi-Chi and Tohoku-Oki earthquakes on scales ranging from that of a single seismic event to several earthquake cycles.

The produced earthquake sequences consist of two types of events: smaller - and more frequent - events that rupture only patch A and larger, model-spanning events that spread over both patches (Figure 3a). All seismic events initiate in patch A which is susceptible to earthquake nucleation due to its rate-weakening properties at low slip rates, and many of them arrest without rupturing patch B. However, occasional events manage to penetrate into patch B and activate coseismic weakening there, essentially changing the patch from (interseismically) stable to (coseismically) unstable. In such model-spanning events, the slip is largest in patch B, due to larger pore-pressure-induced weakening and the associated larger stress drop. Whether dynamic rupture is successful in activating coseismic weakening in patch B depends on a number of factors, which could also be relevant to deeper fault extensions (see the section below) and the creeping segment of the SAF. Such overall pattern of seismic slip is consistent with observations and inferences for the areas of both Tohoku-Oki and Chi-Chi earthquakes. In the Tohoku subduction zone, many Mw 7 to 8 events have occurred on the deeper part of the subduction interface that experienced lower slip in the Tohoku-Oki earthquake (Simons et al., 2011; Figure 2a). Similarly, a series of trench surveys along Chelungpu fault has revealed that earthquakes occur more often in the southern part of the Chi-Chi earthquake source region, which experienced less slip, than in the northern part (Ota et al., 2007). The model dimensions are tailored to the size of the Chi-Chi source, and many model-spanning events in our simulations indeed have peak slip comparable to the 8 m observed in the northern part of the Chi-Chi rupture.

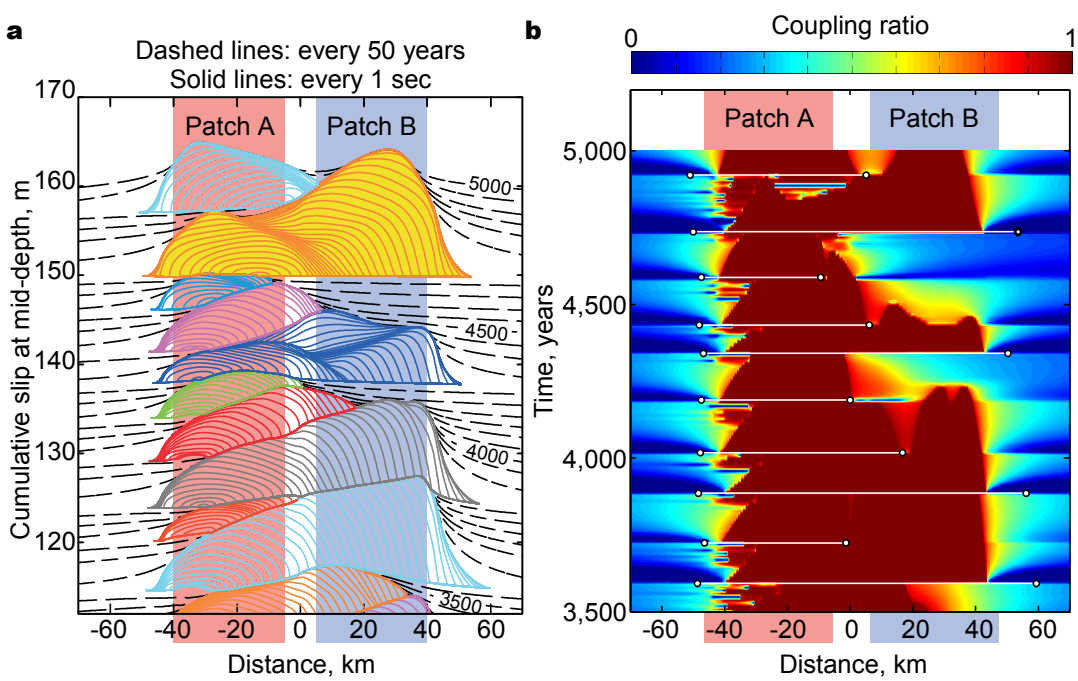

Figure 3. Long-term behavior of the model in terms of earthquake sequences and aseismic slip (Noda and Lapusta, 2013). (a) Cumulative slip distribution along the fault mid-depth. Earthquakes are shown by solid lines plotted every second. Dashed lines represent slow slip

every 50 years, with the numbers indicating the simulated time. Patch A experiences stick-slip. Patch B can both creep and participate in earthquakes, accumulating significant seismic slip. (b) Evolution of fault coupling, with locked segments corresponding to coupling of 1. White lines indicate the extent of earthquake ruptures. Note that patch B can be either creeping or locked before model-spanning seismic events.

Patch B, which combines lab-measured properties that allow for both interseismic creep and rapid coseismic slip, produces a rich variety of behaviors in a single model (Figure 3), from creeping with the long-term convergence rate (i.e. being fully decoupled), to occasionally participating in large seismic events, to being locked (i.e. fully coupled). Such behavior provides a new physical interpretation to the conceptual notion of "conditionally stable" fault behavior (Scholz, 1998). Importantly, right before a seismic event manages to propagate through it, patch B can be creeping (decoupled), in contrast to the notion that large earthquakes rupture mostly locked patches or asperities (Chlieh et al., 2008; Perfettini et al., 2010; Lay, Kanamori and Ruff, 1982). This richness of behavior stands in contrast to patch A, which has relatively simpler stick-slip response.

In addition to capturing the long-term behavior, the model of Noda and Lapusta (2013) simultaneously reproduces the coseismic observations on less pronounced high-frequency radiation from the area of the largest slip in both Chi-Chi and Tohoku-Oki earthquakes (Ma et al., 2003; Meng et al., 2011). Furthermore, the interaction of the two patches can also produce the complex rupture pattern inferred for the Tohoku-Oki earthquake (Ide et al., 2011). Please see Noda and Lapusta (2013) for details.

Depth extent of large earthquakes

It is typically assumed that slip in large earthquakes is confined within the seismogenic zone - often defined by the extent of the background seismicity - with regions below creeping. In terms of rate-and-state friction properties, the locked seismogenic zone and the deeper creeping fault extensions are velocity-weakening (VW) and velocity-strengthening (VS), respectively. Recent studies have suggested that earthquake rupture could penetrate into the deeper creeping regions (Shaw and Wesnousky, 2008), and yet deep slip is difficult to detect due to limited resolution of source inversions with depth. Our modeling of the Tohoku-Oki and Chi-Chi earthquake behavior (Noda and Lapusta, 2013) described in the previous section and our ongoing work (Jiang and Lapusta, 2013) further suggest that such penetration is feasible.

We hypothesize that the absence of concentrated microseismicity at the bottom of the seismogenic zone may point to the existence of deep-penetrating earthquake ruptures. The creeping-locked boundary creates strain and stress concentrations. If it is at the bottom of the VW region, which supports earthquake nucleation, microseismicity should persistently occur at the bottom of the seismogenic zone. Such behavior has been observed, e.g. on the Parkfield segment of the San Andreas Fault (SAF) and the Calaveras fault (Figure 4; Waldhauser et al., 2004, Rubinstein and Beroza, 2007). However, such microseismicity would be inhibited if dynamic earthquake rupture penetrates substantially below the VW/VS transition, which would drop stress in the ruptured VS areas, making them effectively locked. Hence the creeping-locked boundary, with its stress concentration, would be located within the VS area, where earthquake nucleation is inhibited. Indeed, microseismicity concentration at the bottom of the seismogenic zone is not observed for several faults that hosted major earthquakes, such as the Carrizo

segment of the SAF (the site of 1857 Mw 7.9 Fort Tejon earthquake; Figure 4) and Palu-Lake-Hazar segment of the Eastern Anatolian Fault (Bulut et al., 2012; Cetin et al., 2003).

We have confirmed this hypothesis by preliminary simulations which adopt the kind of modeling described in the previous section to this problem (Figure 4). In our model, a VW region is surrounded by VS areas. At the bottom of the VW region, patches of smaller nucleation sizes simulate fault heterogeneity that could lead to microseismicity. On part of the fault, thermally-induced pore fluid pressurization (TP) is effective, as described in section 2.1, leading to enhanced coseismic weakening. In the case where efficient TP is restricted to the VW zone, model-spanning earthquakes arrest quickly in the VS areas, and the creeping-locked boundary reaches the bottom of the VW region early in the earthquake cycle, producing microseismicity (Figure 4, left column). In contrast, if efficient TP extends deeper (5 km deeper in the example), earthquake rupture activates coseismic weakening in the VS areas, penetrating much deeper and generating larger average slip. In this case, the creeping-locked boundary, while moving up-dip with time, is below the VW area throughout the interseismic period, producing no microseismicity (Figure 4, right column).

Hence the absence of concentrated microseismicity at the bottom of the seismogenic zone may point to deeper penetration of large earthquakes. This implies that the 1857 Mw 7.9 Fort Tejon earthquake may have penetrated substantially below the seismogenic zone. The rupture must have been deep enough for the creeping front to remain within the VS area until today, since there is no concentrated microseismicity at the bottom of the seismogenic zone.

This initial success motivates us to continue exploring the issue the deeper penetration of large events, by developing models with more realistic depth-dependent properties.

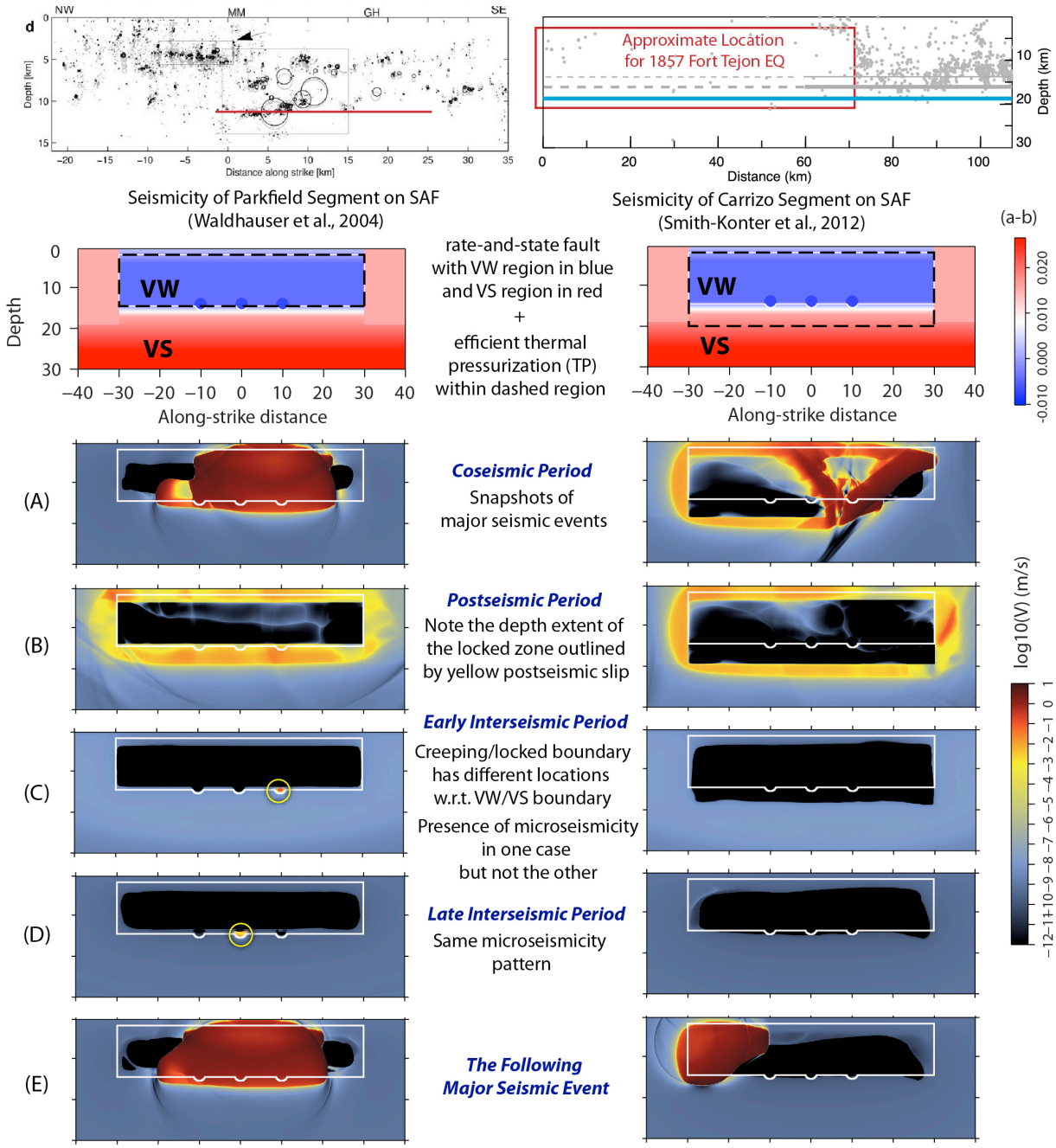

Figure 4. Exploring the possibility of large events penetrating below the seismogenic zone and related observations. First row: the observed microseismicity pattern on Parkfield and Carrizo segment of the San Andreas Fault, only one of which has concentrated microseismicity at the bottom of the seismogenic zone (marked by a red line). The other panels: Slip rate snapshots for two models that qualitatively reproduce such behavior: (I) the case in which efficient thermal pressurization (TP) of pore fluid during earthquake rupture does not occur below VW/VS boundary (left); (II) the case in which efficient TP could be activated deeper (right). Black indicates locked zones, blue indicates creep with the imposed plate rate, and red indicates seismic slip. While small events (marked by

yellow circles) at the rheological transition occur throughout interseismic period in case (I), the fault is void of such small events in case (II).

REFERENCES

Andrews, D. J., A fault constitutive relation accounting for thermal pressurization of pore fluid, *J. Geophys. Res*., **107**(B12), 2363, doi:10.1029/2002JB001942, 2002.

Barbot, S., N. Lapusta, and J.-P. Avouac, Under the hood of the earthquake machine: Toward predictive modeling of the seismic cycle, *Science*, *336*(6082), 707–710, doi:10.1126/science.1218796, 2012.

Beeler, N. M., and T. E. Tullis, Constitutive relationships for fault strength due to flash-heating. In: *2003 SCEC Annual Meeting Proceedings and Abstracts*, vol. 13, p. 66. Los, Angeles: Southern California Earthquake Center, Univ. of Southern California, 2003.

Beeler, N. M., T. E. Tullis, and D. L. Goldsby , Constitutive relationships and physical basis of fault strength due to flash-heating, *J. Geophys. Res*., **113**, B01401, doi:10.1029/2007JB004988, 2008.

Bizzarri, A., and M. Cocco, A thermal pressurization model for the spontaneous dynamic rupture propagation on a three-dimensional fault: 1. Methodological approach, *J. Geophys. Res*., **111**, B05303, doi:10.1029/2005JB003862, 2006a.

Bizzarri, A., and M. Cocco, A thermal pressurization model for the spontaneous dynamic rupture propagation on a three-dimensional fault: 2. Traction evolution and dynamic parameters, *J. Geophys. Res*., **111**, B05304, doi:10.1029/2005JB003864, 2006b.

Blanpied, M. L., D. A. Lockner and J. D. Byerlee, Fault stability inferred from granite sliding experiments at hydrothermal conditions, *Geophys. Res. Letters*, **18** (4), 609-612, 1991.

Blanpied, M. L., D. A. Lockner and J. D. Byerlee, Frictional slip of granite at hydrothermal conditions, *J. Geophys. Res*., **100**, 13045-13064, 1995.

Bulut, F., M. Bohnhoff, T. Eken, C. Janssen, T. Kılıç, and G. Dresen, The East Anatolian Fault Zone: Seismotectonic setting and spatiotemporal characteristics of seismicity based on precise earthquake locations, *J. Geophys. Res.*, *117*(B7), B07304, doi:10.1029/2011JB008966, 2012.

Cetin, H., H. Güneyli, and L. Mayer, Paleoseismology of the Palu–Lake Hazar segment of the East Anatolian Fault Zone, Turkey, *Tectonophysics*, *374*(3-4), 163–197, doi:10.1016/j.tecto.2003.08.003, 2003.

Chen, T., and N. Lapusta , Scaling of small repeating earthquakes explained by interaction of seismic and aseismic slip in a rate and state fault model, *J. Geophys. Res.*, 114, B01311, doi:10.1029/2008JB005749, 2009.

Chen, T., and N. Lapusta, Interaction of small repeating earthquakes in a rate and state fault model, *AGU Fall Meeting*, T33B-2255, 2010.

Chlieh, M., Avouac, J.-P., Sieh, K., Natawidjaja, D. H. & Galetzka, J. Heterogeneous coupling of the Sumatran megathrust constrained by geodetic and paleogeodetic measurements. *J. Geophys. Res.* **113**, doi:10.1029/2007JB004981, 2008.

Dieterich, J. H., Modeling of rock friction- 1 Experimental results and constitutive equations, *J. Geophys. Res.*, **84**, 2161-2168, 1979.

Dieterich, J. H., Constitutive properties of faults with simulated gouge, in *Mech. Beh. Crustal Rocks*, Geophys. Monogr. Ser., **24**, ed. by N. L. Carter, M. Friedman, J. M. Logan and D. W. Stearns, AGU, Washington, DC, 103-120, 1981.

Dieterich, J. H. Applications of rate- and state-dependent friction to models of fault slip and earthquake occurrence. In Kanamori, H. (ed.) *Treatise on Geophysics*, **4**, chap. 4, 107–129 (Elsevier, Amsterdam, 2007).

Goldsby, D. L., and T. E. Tullis, Flash heating/melting phenomena for crustal rocks at (nearly) seismic slip rates. In: *2003 SCEC Annual Meeting Proceedings and Abstracts*, vol. 13, p. 98-99. Los Angeles: Southern California Earthquake Center, Univ. of Southern California, 2003.

Ide, S., Baltay, A. & Beroza, G. C. Shallow dynamic overshoot and energetic deep rupture in the 2011 Mw 9.0 Tohoku-Oki earthquake. *Science* **332**, 1426–1429, doi:10.1126/science.1207020, 2011.

Lapusta, N., and Y. Liu, 3D boundary-integral modeling of spontaneous earthquake sequences and aseismic slip, accepted for publication, *J. Geophys. Res.*, 2009.

Lapusta, N., J. R. Rice, Y. Ben-Zion, and G. Zheng, Elastodynamic analysis for slow tectonic loading with spontaneous rupture episodes on faults with rate- and state-dependent friction, *J. Geophys. Res*. 105, 23765-23789, 2000.

Lay, T., Kanamori, H. and L. Ruff, The asperity model and the nature of large subduction zone earthquakes. *Earthquake Prediction Research* **1**, 3–71, 1982.

Ma, K. F., Song T. R., Lee S. J. and H. Wu, Spatial slip distribution of the September 20, 1999, Shi-Shi, Taiwan, earthquake (Mw 7.6) --Inverted from teleseismic data, *Geophys, Res. Lett.* **27**, doi:10.1029/2000GL011393, 2000.

Ma, K. F., Brodsky E., Mori J., Ji C., Song T. R. and H. Kanamori, Evidence for fault lubrication during the 1999 Chi-Chi, Taiwan, earthquake (Mw7.6). *Geophys. Res. Lett.* **30**, doi:10.1029/2002GL015380, 2003.

Noda, H., E. M. Dunham, and J. R. Rice, Earthquake ruptures with thermal weakening and the operation of major faults at low overall stress levels, *J. Geophys. Res.*, *114*, B07302, doi:10.1029/2008JB006143, 2009.

Noda, H., and N. Lapusta, Three-dimensional earthquake sequence simulations with evolving temperature and pore pressure due to shear heating: Effect of heterogeneous hydraulic diffusivity, *J. Geophys. Res.*, *115*(B12), doi:10.1029/2010JB007780, 2010.

Noda, H., and N. Lapusta, Stable creeping fault segments can become destructive as a result of dynamic weakening, *Nature*, 1–6, doi:10.1038/nature11703, 2013.

Ota, Y. *et al.* Low-angle reverse faulting during two earthquakes on the northern part of the Chelungpu fault, deduced from the Fengyuan trench, central Taiwan. *Terr. Atmos. Ocean. Sci.* **18**, 55–66, 2007.

Perfettini, H. *et al.* Seismic and aseismic slip on the central Peru megathrust. *Nature* **465**, 78–8. Doi:10.1038/nature09062, 2010.

Rice, J. R., Heating and weakening of faults during earthquake slip, *J. Geophys. Res*., doi:10.1029/2005JB004006, 2006.

Rice, J. R., N. Lapusta, and K. Ranjith, Rate and state dependent friction and the stability of sliding between elastically deformable solids, *J. Mech. Phys. Solids* 49, 1865-1898, 2001.

Rubinstein, J. L., and G. C. Beroza, Full waveform earthquake location: Application to seismic streaks on the Calaveras Fault, California, *J. Geophys. Res.*, *112*(B5), doi:10.1029/2006JB004463, 2007.

Ruina, A. L., Slip instability and state variable friction laws, *J. Geophys. Res*., **88**, 10359-10370, 1983.

Scholz, C. H. Earthquakes and friction laws. *Nature* **391**, 37–42, 1998.

Sibson, R. H., Interaction between temperature and pore-fluid pressure during earthquake faulting and a mechanism for partial or total stress relief, *Nature*, **243**, 66–68, 1973.

Simons, M. et al., The 2011 Magnitude 9.0 Tohoku-Oki Earthquake: Mosaicking the Megathrust from Seconds to Centuries, *Science*, *332*(6036), 1421–1425, doi:10.1126/science.1206731, 2011.

Shaw, B. E., and S. G. Wesnousky, Slip-Length Scaling in Large Earthquakes: The Role of Deep-Penetrating Slip below the Seismogenic Layer, *Bull. Seismol. Soc. Amer.*, *98*(4), 1633–1641, doi:10.1785/0120070191, 2008.

Tanikawa, W. & Shimamoto, T. Frictional and transport properties of the Chelungpu fault from shallow borehole data and their correlation with seismic behavior during the 1999 Chi-Chi earthquake. *J. Geophys. Res.* **114**, B01502, doi:10.1029/2008JB005750, 2009.

Tsutsumi, A. & Shimamoto, T. High velocity frictional properties of gabbro. *Geophys. Res. Lett.* **24**, 699–702, 1997.

Waldhauser, F., W. L. Ellsworth, D. P. Schaff, and A. Cole, Streaks, multiplets, and holes: High-resolution spatio-temporal behavior of Parkfield seismicity, *Geophys. Res. Lett*., doi:10.1029/2004GL020649, 2004.